ACOUSTICS 2012

Static correction of acoustic models with application to vibro-acoustic coupling

J.-M. Lagache[a] and S. Assaf[b]

[a]PSA Peugeot - Citroën, Centre Technique de la Garenne Colombes Case courrier LG098 18, rue des Fauvelles 92256 La Garenne Colombes cedex
[b]ESTACA, 34 rue Victor Hugo, 92532 Levallois Perret Cedex, France
jeanmarie.lagache@mpsa.com

A direct method,- termed "Method of Orthocomplement",- of determination of modal remainders in truncated modal series, in structural or acoustic analyses, has been proposed by the authors, leading to explicit expressions of the response of a free-floating mechanical system or of an acoustic cavity, by explicit "accelerated" modal formulae including *static terms* and *accelerated modal series*. The resulting formulae are recalled in the paper, with a special attention to the pseudo-inversion techniques required by the singular static terms. Since the coupling of an acoustic cavity results from the reduction of the acoustic dynamic stiffness to generalized degrees of freedom defined by the coupling matrix, it will be shown that applying the preceding formulae to vibro-acoustic coupling leads to two possible methods : a "low frequency" method based on the algebraic computation of static terms, which delivers *added stiffness and mass matrices* to be used from the Helmholtz 0Hz frequency to the first non-zero acoustic frequency ; a general "high frequency" method where the preceding static terms are complemented by a reasonable number of cavity modes.

1 Introduction

In this paper, modified "accelerated" modal formulae are applied to the effective solution, through pure finite-element modeling of both structural and acoustic parts, of vibro-acoustic coupling problems. In contrast with more widespread general methods, [1,2] , a one-variable Helmholtz fluid formulation is retained, with the main advantage that, besides the possibility of using simple laptop computers, the connection with physical concepts remain accessible, which clearly enhances a better understanding of the specificities of vibro-acoustics by comparison with ordinary coupling of structural subsystems.

"Accelerated" modal formulae are presented in Part 2 of the paper, with a special emphasis on pseudo-inversion operations, that are strictly required by the singularities of structural matrices in the general case of free-floating structures or acoustic cavities, and unfortunately make the whole difficulty of the subject. Detailed proofs should be found, by example, in ref. [3], and technical details on pseudo-inversion in ref [4]. In addition, it should be remarked that equivalent results can be obtained in an implicit form through appropriate Ritz-Galerkin transformations [5,6]. From the practical point of view, one will find at the end of the section a short MatLab® script that can be used to change abstract considerations on pseudo-inverse operators into effective operations on structural or acoustic matrices.

In parallel with applications to Structural Dynamics, various applications to the calculation of acoustic responses and receptances have been proposed by the authors [7]. Part 3 of the paper develops a first application to vibro-acoustic coupling, with convincing test examples in Part 4.

2 Accelerated modal formulae

2.1 General formulae

Consider two positive NxN symmetric matrices K, M , where M is a regular matrix while K is a degenerate matrix of rank N-s - typically a stiffness and a mass matrix in free floating conditions – and suppose that the generalized eigenvalues and eigenvectors of matrix K with respect to M have been properly extracted through an appropriate modal analysis. The NxN matrix of mass-normalized modes, $\boldsymbol{\Psi}$, being split up in a $\sigma \times N$ modal matrix, $\boldsymbol{\Psi}_0$, related to modes at zero frequency, and a $(N-\sigma)\times N$, modal matrix, $\boldsymbol{\Psi}_+$, corresponding to modes at strictly positive frequencies, it has been shown in ref. [3] that:

$$\begin{aligned}\left(\boldsymbol{K}-\omega^2\boldsymbol{M}\right)^{-1} &= -\frac{\boldsymbol{\Psi}_0\boldsymbol{\Psi}_0^{\mathsf{T}}}{\omega^2}+\dots\\ &\left(\boldsymbol{1}-\boldsymbol{\Pi}_M\right)\left(\lambda\boldsymbol{\Pi}+\boldsymbol{K}\right)^{-1}\left(\boldsymbol{1}-\boldsymbol{\Pi}_M^{\mathsf{T}}\right)+\dots\\ &\boldsymbol{\Psi}_+\ \boldsymbol{diag}\left(\left\{\frac{\omega^2}{\omega_m^{\ 2}}\frac{1}{\omega_m^{\ 2}-\omega^2}\right\}_{m=\sigma+1,\dots N}\right)\boldsymbol{\Psi}_+^{\mathsf{T}}\end{aligned} \qquad (1)$$

with the consequence that for any localization or combination matrix $\boldsymbol{P}$:

$$\begin{aligned}\boldsymbol{P}\left(\boldsymbol{K}-\omega^2\boldsymbol{M}\right)^{-1}\boldsymbol{P}^{\mathsf{T}} &= -\frac{\boldsymbol{P\Psi}_0\left(\boldsymbol{P\Psi}_0\right)^{\mathsf{T}}}{\omega^2}+\dots\\ &\boldsymbol{P}\left(\boldsymbol{1}-\boldsymbol{\Pi}_M\right)\left(\lambda\boldsymbol{\Pi}+\boldsymbol{K}\right)^{-1}\left(\boldsymbol{1}-\boldsymbol{\Pi}_M^{\mathsf{T}}\right)\boldsymbol{P}^{\mathsf{T}}+\dots \quad (2)\\ &\boldsymbol{P\Psi}_+\ \boldsymbol{diag}\left(\left\{\frac{\omega^2}{\omega_m^{\ 2}}\frac{1}{\omega_m^{\ 2}-\omega^2}\right\}_{m=\sigma+1,\dots N}\right)\left(\boldsymbol{P\Psi}_+\right)^{\mathsf{T}}\end{aligned}$$

The preceding formula obviously needs for some clarifications.

- The first term in the right hand side of Eq. (2) is clearly the singular contribution of 0Hz modes
- The second term describes in structural applications elastic deformation under combinations of external and inertial forces, and is ordinarily referred to as "Inertia Relief Contribution". It results from delicate pseudo-inversion techniques that are fully detailed in refs. [3,4] . Note that $\boldsymbol{\Pi}$ and $\boldsymbol{\Pi}_M$, respectively stand for the Euclidian and M-projectors to the nullspace, $\ker\boldsymbol{K}$, spanned by $\boldsymbol{\Psi}_0$. Also note that λ denotes an arbitrary non zero number, whose presence is essential to perform the centre inversion, but whose value has curiously no influence on the overall result (see details in refs [3,4]).
- The third term, at last, only differs from an ordinary modal summation by the "accelerating" factor $\omega^2/\omega_m^{\ 2}$ that affects each contribution. This obviously tends, at a given frequency, to

drastically minimize the contributions of high order modes, and thus the truncation error.

2.2 Theoretical comments

An indefectible connection exists between truncation corrections and exactness at 0Hz, and, it is important to note that the first two terms in decompositions (1) or (2) are indeed the exact first two coefficients in the Laurent expansion of the considered receptances at 0Hz.

The whole affair is indeed in the progressive transformation of ordinary modal representations in the form

$$\left(\boldsymbol{K}-\omega^2\boldsymbol{M}\right)^{-1}=\boldsymbol{\Psi}\ \boldsymbol{diag}\left(\left\{\frac{1}{\omega_m{}^2-\omega^2}\right\}_{m=1,\dots N}\right)\boldsymbol{\Psi}^{\mathsf{T}} \quad (3)$$

A step-by-step direct analysis of modal remainders leading to that transformation,- termed "method of orthocomplement",- is fully detailed in ref. [3] .

Complements on inertial and inertia relief contributions can also be found in ref. [4] .

Although that result has not still been published, note that appropriate Ritz-Galerkin transformations have been verified to implicitly lead to the same result.

2.3 Practical computations

If $\boldsymbol{S}$ denotes an arbitrary spanning matrix of $ker\,\boldsymbol{K}$ - by instance $\boldsymbol{S}=\boldsymbol{\Psi}_0$ - projectors $\boldsymbol{\Pi}$ and $\boldsymbol{\Pi}_M$ can be expressed as [3,4]:

$$\begin{cases}\boldsymbol{\Pi}=\boldsymbol{S}\left(\boldsymbol{S}^T\boldsymbol{S}\right)^{-1}\boldsymbol{S}^T\\ \boldsymbol{\Pi}_M=\boldsymbol{S}\left(\boldsymbol{S}^T\boldsymbol{M}\,\boldsymbol{S}\right)^{-1}\boldsymbol{S}^T\boldsymbol{M}\end{cases} \quad (4)$$

From this, the inertia relief coefficient, say $\boldsymbol{a}_1$, can be easily derived ; while, the inertial coefficient,

$$\boldsymbol{a}_0=\boldsymbol{P\Psi}_0\left(\boldsymbol{P\Psi}_0\right)^{\mathsf{T}}=\boldsymbol{P\Psi}_0\boldsymbol{\Psi}_0{}^{\mathsf{T}}\boldsymbol{P}^{\mathsf{T}} \quad (5)$$

can be seen [3,4] to be given by the general expression :

$$\boldsymbol{a}_0=\boldsymbol{P}\,\boldsymbol{S}\left(\boldsymbol{S}^{\mathsf{T}}\boldsymbol{M}\,\boldsymbol{S}\right)^{-1}\boldsymbol{S}^{\mathsf{T}}\boldsymbol{P}^{\mathsf{T}} \quad (6)$$

that perfectly coincides with expression (5) when $\boldsymbol{S}=\boldsymbol{\Psi}_0$ since, in that case, $\boldsymbol{\Psi}_0{}^{\mathsf{T}}\boldsymbol{M}\boldsymbol{\Psi}_0=\boldsymbol{1}$.

The practical computation of the first two terms in expression (2) can thus be performed by the simple MatLab script that follows, while the third term can be easily assembled since it only differs from an ordinary modal summation by the acceleration factor $\omega^2/\omega_m{}^2$.

```
%-----------------------------------------
  Given K , M and a localization matrix P
%-----------------------------------------
S=null(full(K)) ;          % kernel of K
N=size(K,1) ;
PI=S*(S.'*S)\S.' ;         % PI-projector
PM=S*((S.'*M*S)\S.'*M)) ; % M-projector
UN=sparse(eye(N)) ;
UNPM=UN-PM ;     % complementary M-projector
PS=P*S ;
P1PM=P*UNPM ;
lambda=trace(K)/N ; %conditioning of pinv
ISVD=lambda*PI+K ;
a0=S*((S'*M*S)\PS.') ;
a1=UNPM*(ISVD\P1PM.') ;;
a0=P*a0 ;   % inertial coefficient in Eq.(2)
a1=P*a1 ;   % inertia relief term in Eq.(2)
```

3 Vibro-acoustic coupling

3.1 One-variable fluid formulation and coupling matrix

The variational formulation and finite-element discretization of vibro-acoustic models lead to hybrid linear systems, linking nodal vectors of structural displacements $\boldsymbol{U}$ and acoustic pressures, $\boldsymbol{P}$, to the vectors of structural and acoustic excitations, $\boldsymbol{F}$, $\boldsymbol{D}$, through equations in the form :

$$\begin{pmatrix}\boldsymbol{K}-\omega^2\boldsymbol{M} & \boldsymbol{C}\\ \boldsymbol{C}^{\mathsf{T}} & \dfrac{\boldsymbol{H}}{\rho_f\omega^2}-\dfrac{\boldsymbol{Q}}{\rho_f c^2}\end{pmatrix}\begin{Bmatrix}\boldsymbol{U}\\ \boldsymbol{P}\end{Bmatrix}=\begin{Bmatrix}\boldsymbol{F}\\ \boldsymbol{D}\end{Bmatrix} \quad (7)$$

where $\boldsymbol{K}$, $\boldsymbol{M}$ are the stiffness and mass matrices of the structural part ; $\boldsymbol{H}$, $\boldsymbol{Q}$, the <u>normalized</u> fluid matrices, in use to approximate volume integrals in the form $\int_{\Omega_f}\nabla p.\nabla\varpi\,dV\approx\mathbf{p}\ \mathbf{H}\,\boldsymbol{\varpi}$, $\int_{\Omega_f}p.\varpi\,dV\approx\mathbf{p}\ \mathbf{Q}\,\boldsymbol{\varpi}$; and $\boldsymbol{C}$, the "coupling matrix" classically used [2] to approximate surface integrals in the form $\int_{\partial\Omega_f}p\,u_n ds\approx\boldsymbol{u_n}^{\mathsf{T}}\boldsymbol{C}\ \boldsymbol{p}$.

Provided the attention is focused on the mechanical response of the structural part, and provided there are no acoustic sources, Eq. (7) can readily be reduced to:

$$\left[\boldsymbol{K}-\omega^2\boldsymbol{M}-\rho_f\omega^2\boldsymbol{C}\left(\boldsymbol{H}-\frac{\omega^2}{c^2}\boldsymbol{Q}\right)^{-1}\boldsymbol{C}^{\mathsf{T}}\right]\boldsymbol{U}=\boldsymbol{F} \quad (8)$$

Because $\boldsymbol{H}$ and $\boldsymbol{Q}$ have exactly the same algebraic properties as the $\boldsymbol{K}$ and $\boldsymbol{M}$ structural matrices, it is clear that formulae (2) can be applied, using the coupling matrix $\boldsymbol{C}$ in place of $\boldsymbol{P}$, and the generalized eigenvalues and eigenvectors of $\boldsymbol{H}$ with respect to $\boldsymbol{Q}$,or in other words, the rigid cavity modes and frequencies, in place of the structural modes and eigenfrequencies.

Before proceeding to that substitution, it is important to note that despite of a total algebraic similarity, structural and Helmholtz fluid matrices are physically antagonistic entities, respectively of the rigidity type and of the mobility type. In particular, modes refer in the former case to states of maximum compliance, and in the latter case to states of maximum rigidity. That exchange of displacement and force variables is the specificity of Helmholtz vibro-acoustic coupling and can lead unfortunately to erroneous ideas – like hoping to observe the Helmholtz mode on the coupled structural system – and also of unforeseen difficulties – like the absence of efficient acoustic static corrections in most commercial finite-element codes, that probably takes its origin in the fact that the projector term in Eq. (2) although its expression remains perfectly valid in the dual acoustic background, cannot be easily given as an inertia relief term and thus remains hardly accessible to current engineering considerations.

3.2 Low frequency added stiffness and mass method

Provided acoustic modal contributions of the third term of Eq. (2) remain negligible, namely in the low frequency range between the 0Hz Helmholtz frequency and the first non-zero cavity frequency, the considered equation can be approximately developed as :

$$\boldsymbol{C}\left(\boldsymbol{H}-\frac{\omega^2}{c^2}\boldsymbol{Q}\right)^{-1}\boldsymbol{C}^{\mathsf{T}}=-c^2\frac{\boldsymbol{a}_0}{\omega^2}+\boldsymbol{a}_1+\cdots \tag{9}$$

with

$$\begin{cases}\boldsymbol{a}_0=\boldsymbol{C}\,\boldsymbol{S}\left(\boldsymbol{S}^{\mathsf{T}}\boldsymbol{Q}\,\boldsymbol{S}\right)^{-1}\boldsymbol{S}^{\mathsf{T}}\boldsymbol{C}^{\mathsf{T}}\\ \boldsymbol{a}_1=\boldsymbol{C}\left(\boldsymbol{1}-\boldsymbol{\Pi}_Q\right)\left(\lambda\boldsymbol{\Pi}+\boldsymbol{H}\right)^{-1}\left(\boldsymbol{1}-\boldsymbol{\Pi}_Q^{\mathsf{T}}\right)\boldsymbol{C}^{\mathsf{T}}\end{cases} \tag{10}$$

where $\boldsymbol{S}$ is a spanning matrix of $ker\,\boldsymbol{Q}$, and the computation of projectors is now greatly simplified by the fact that this nullspace in acoustic applications is a 1-dimensional vector space of constant vectors [7].

There is no difficulty to introduce *added stiffness* and *mass* matrices

$$\begin{cases}\delta\boldsymbol{K}=\rho_f c^2\boldsymbol{a}_0\\ \delta\boldsymbol{M}=\rho_f\boldsymbol{a}_1\end{cases} \tag{11}$$

to simply write the coupled equation of motion of the structural part as

$$\left[\left(\boldsymbol{K}+\delta\boldsymbol{K}\right)-\omega^2\left(\boldsymbol{M}+\delta\boldsymbol{M}\right)\right]\boldsymbol{U}=\boldsymbol{F} \tag{12}$$

Assembling and solving this equation is termed in the following example "the low frequency" or "added stifness and mass method". The method is valid between 0Hz and the first non-zero cavity eigenfrequency. The contribution of the paper is in the expressions (10),(11) of coefficients in terms of projectors and in their interpretation as Laurent coefficients relative to the coupling matrix.

3.3 Accelerated modal high frequency method

After an adequate renormalization of acoustic modal entities,- that is necessitated by the presence in a-dimensional equations of terms ρ_f, c, and wave numbers ω/c,- there is no difficulty to deduce from (2) something like that :

$$\begin{aligned}&\boldsymbol{C}\left(\boldsymbol{H}-\frac{\omega^2}{c^2}\boldsymbol{Q}\right)^{-1}\boldsymbol{C}^{\mathsf{T}}=-c^2\frac{\boldsymbol{a}_0}{\omega^2}+\boldsymbol{a}_1+\cdots\\ &\sum_{m=2}^{n}\frac{\omega^2}{\omega_m^{\ 2}}\frac{1}{\omega_m^{\ 2}-\omega^2}\boldsymbol{\Psi}_C^{\langle m\rangle}\boldsymbol{\Psi}_C^{\langle m\rangle\mathsf{T}}+\cdots\end{aligned} \tag{13}$$

where,- $\boldsymbol{\Psi}^{\langle m\rangle}$ being an adequate system of renormalized cavity modes at frequencies ω_m ,- $\boldsymbol{\Psi}_C^{\langle m\rangle}=\boldsymbol{C}\boldsymbol{\Psi}^{\langle m\rangle}$ denotes the restriction of these modes to the generalized dofs that are defined by the coupling matrix.

Substituting that expression in Eq. (8) then brings the following correction to the low frequency approximation of the preceding paragraph:

$$\begin{bmatrix}\left(\boldsymbol{K}+\delta\boldsymbol{K}\right)-\omega^2\left(\boldsymbol{M}+\delta\boldsymbol{M}\right)\cdots\\ \cdots-\rho_f\omega^4\sum_{m=2}^{n}\frac{1}{\omega_m^{\ 2}}\frac{1}{\omega_m^{\ 2}-\omega^2}\boldsymbol{\Psi}_C^{\langle m\rangle}\boldsymbol{\Psi}_C^{\langle m\rangle\mathsf{T}}\end{bmatrix}\boldsymbol{U}=\boldsymbol{F} \tag{14}$$

That way of doing is termed here "accelerated modal high frequency method". It will be shown on examples that it can be used without any restriction on the frequency range.

4 Test examples

4.1 Coupling of aluminium and steel plates to an acoustic cube

The proposed coupling methods have been first tested on the 1mx1mx1m acoustic cube of Fig. 1. The cavity is filled up with air at ambient conditions. All walls are kept rigid, at the exception of the upper face, which is first coupled with a simply supported 1mx1m aluminium plate of 5.10^{-3}m width, and second to a more rigid steel plate of the same dimensions .

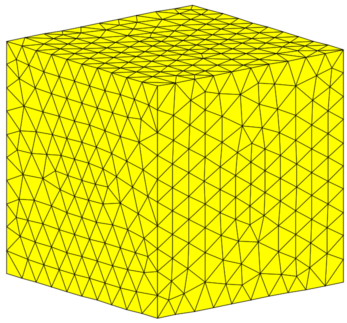

Figure 1: Meshed skin of the first test example (1mx1mx1m cube filled up with air)

The acoustic mesh comprises 4930 CTETRA elements corresponding to 1193 acoustic nodes and nodal pressures. The first acoustic non zero cavity resonance is found at

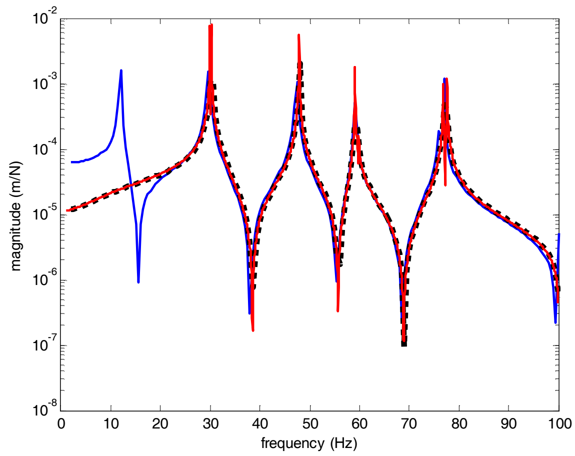

Figure 2: [0,100Hz]-pointwise receptance on an aluminium plate coupled with an acoustic cube : *added stiffness and mass* (-) , *exact* (…), *in vacuo* (-)

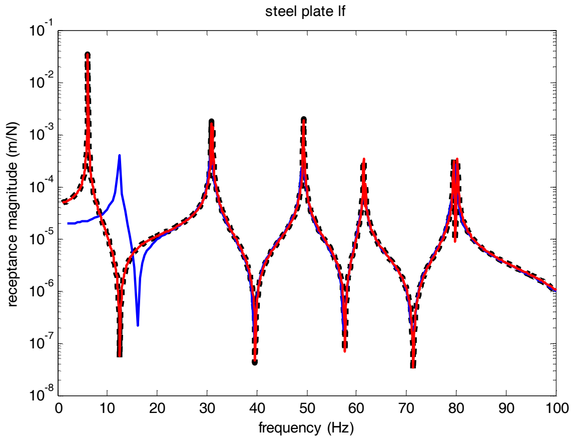

Figure 3: [0,100Hz]-pointwise receptance on a steel plate coupled with an acoustic cube : *added stiffness and mass* (-) , *exact* (**…**), *in vacuo* (-)

170.9Hz. Structural meshes comprises 135 nodes coinciding with acoustic nodes at the upper face of the cube. Finite element models of the plates are reduced to 405 dofs, corresponding to normal deflections and in-plane rotations.

Figs. 2 and 3 show the reconstitutions in the range [0,100Hz] of pointwise receptances at the surface of the coupled plates by the low frequency approximation(12). Results are in perfect agreement with direct computations. Blue lines on the figures correspond to receptances *in vacuo* . It is interesting to note that the first *in vacuo* mode of the aluminium plate fades out after coupling, , literally stuck by the rigidity of the Helmholtz mode. This is not the case for the stronger steel plate for which the *in vacuo* mode changes itself to a coupled mode at a lower frequency.

The first acoustic non zero cavity mode lying at 170.9Hz, it should be clear from theoretical considerations of Section 3 that in the considered [0,100Hz] range no other acoustic perturbations than the preceding ones can be expected or observed.

To show such perturbations, Figs. 4 and 5 proposes reconstitutions of the preceding pointwise receptances in

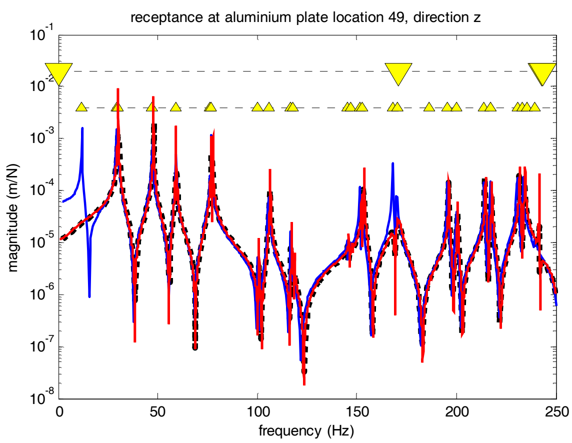

Figure 4: [0,250Hz]-pointwise receptance on an aluminium plate coupled with an acoustic cube : *hf method* (-) , *exact* (**…**), *in vacuo* (-) ; *acoustic* (v) and *structural* (^) frequencies

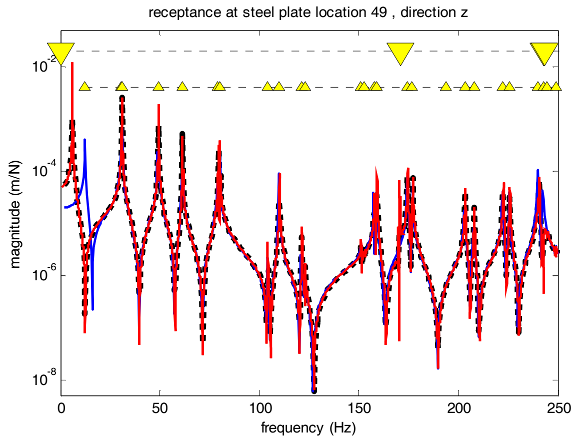

Figure 5: [0,250Hz]-pointwise receptance on a steel plate coupled with an acoustic cube : *hf method* (-) , *exact* (**…**), *in vacuo* (-) ; *acoustic* (v) and *structural* (^) frequencies

the range [0,250Hz], using the accelerated modal “high frequency formulae” (14). Three cavity frequencies, and due to the symmetries of the cube, eight cavity modes are present in the considered frequency band : the Helmholtz mode at 0Hz, 3 modes at 170.9 Hz and 3 other modes at 243 Hz.

One can observe a perfect agreement of accelerated modal calculations with direct resolution. Perturbations of *in vacuo* responses, are concentrated around the three cavity frequencies, and visibly affect the structural modes in frequency coincidence. Although the example may seem extremely simple, various sorts of perturbations can be observed with the steel or aluminium plates, which seems to generalize what was already detected with the Helmholtz mode.

4.2 Coupling of an aluminium plate to a parallelepipedal acoustic cavity

In the second test example of Fig. 6, the preceding cube is dilated to a 1mx1mx4m parallelepiped,- meshed up with 28605 CTETRA elements and 6370 nodes ,- still filled up with air and coupled on one of its square faces to the same simply supported 1mx1m aluminium plate as before.

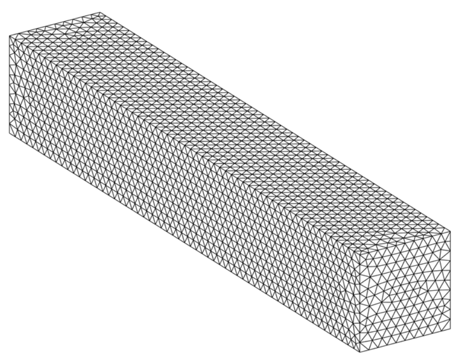

Figure 6: Meshed skin of the second test example (1mx1mx4m parallelepiped filled up with air)

As a consequence, the first non-zero acoustic eigenfrequency, which was about 170.9 Hz in the first example, now falls to 28.4Hz, with the major consequence

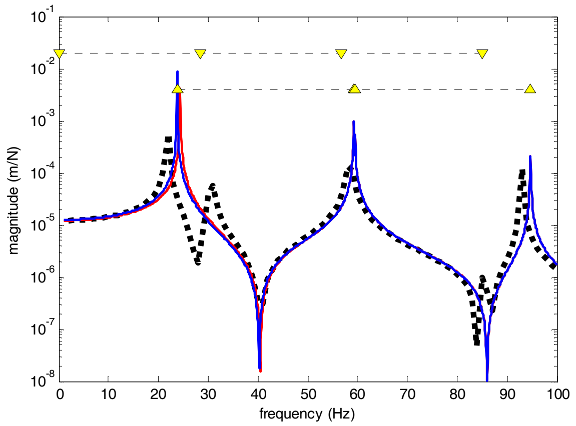

Figure 7: [0,100Hz]-pointwise receptance on an aluminium plate coupled with an acoustic parallelepiped: *added stiffness and mass* (-) , *exact* (…), *in vacuo* (-) ; *acoustic* (v) and *structural* (^) frequencies.

that the low frequency added stiffness and mass method fails to correctly render the vibro-acoustic coupling in the [0;100Hz] band, as illustrated on Fig. 7 .

Apart from slight disturbances that take their origin in some imprecisions in the finite element code used to compute the exact solution, Fig. 8 shows an almost perfect concordance of the accelerated modal method (14) with quasi-exact computations.

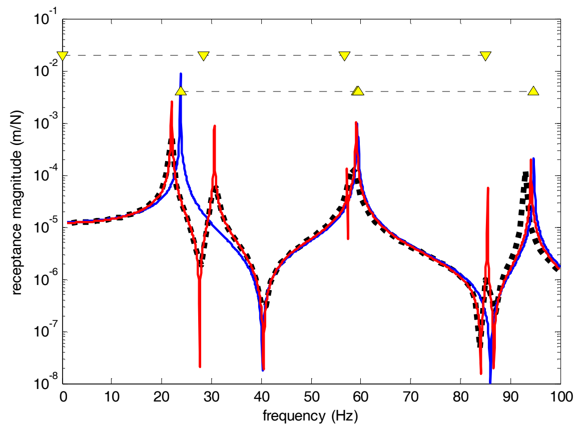

Figure 8: [0,100Hz]-pointwise receptance on an aluminium plate coupled with an acoustic parallelepiped : *hf method* (-) , *exact* (…), *in vacuo* (-) ; *acoustic* (v) and *structural* (^) frequencies.

Finally, Fig. 9 shows how the *in vacuo* behavior of the plate should be perturbed by acoustic coupling in the [0,250Hz] frequency range.

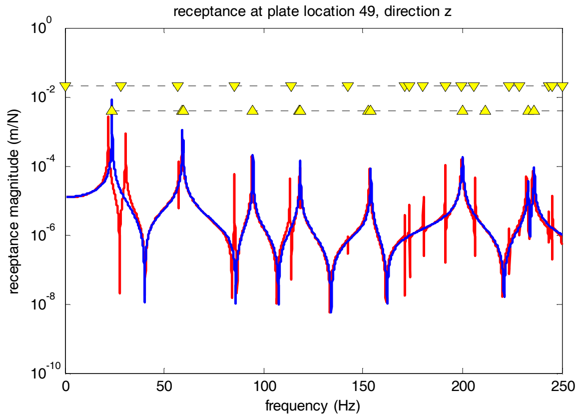

Figure 9: [0,250Hz]-pointwise receptance on an aluminium plate coupled with an acoustic parallelepiped: *hf method* (-), *in vacuo* (-) ; *acoustic* (v) and *structural* (^) frequencies.

5 Conclusion

The authors sincerely hope to have shown that the use of apparently esoteric mathematical considerations has brought a very practical, concise and efficient technique of vibro-acoustic coupling, whose main advantage,- especially for tutorial purposes,- is to remain very close to Physics.

References

[1] R.Ohayon,C.Soize, *Structural Acoustics and Vibration*, Academic Press, San Diego (1998).ISBN 0-12-524945-4

[2] M.A. Hamdi, « Méthodes de discrétisation par éléments finis et éléments finis de frontière » in C. Lesueur, *Rayonnement acoustique des structures,* Eyrolles, Paris (1988) in french

[3] J-M.Lagache, S.Assaf & C.Schulte, "Finite element synthesis of structural or acoustic receptances in view of practical design applications", *Journal of Sound and Vibration* (2008) 310:313-351

[4] J-M.Lagache, S.Assaf , "Elimination of internal structural variables through explicit Taylor-Laurent model reduction, with applications to damped sandwich plates", *Acta Acustica* (2012) under press

[5] R.R. Craig, Jr., A.J. Kurdila, *Fundamentals of Structural Dynamics,* 2nd ed . John Wiley & Sons, Inc., Hoboken, New Jersey, (2006).

[6] D. de Klerk, D.J. Rixen, S.N. Voormeeren, "General Framework for Dynamic Substructuring: History, Review, and Classification of Techniques", *AIAA J* , Vol. **46**, N° **5**, (2008)

[7] S.Assaf, J-M.Lagache , "Modal Finite element synthesis of acoustic boundary receptances", *Mécanique & Industries*, **9** , 579-588 (2008)